Research Article Vol. 33, No. 16 / 11 Aug 2025 / Optics Express 33446
Optics EXPRESS

Photon statistics of one- and two-photon subtracted states at telecom wavelength reconstructed via direct detection

P. Ercolano,[1,*] A. Porzio,[2] M. Ejrnaes,[3,4] D. Salvoni,[4,5] C. Bruscino,[1] M. Peluso,[1] J. Huang,[6] C. Zhang,[1,4,5] H. Li,[6] L. You,[6] L. Parlato,[1] and G. P. Pepe[1]

[1]*Dip. di Fisica "E. Pancini", Università degli Studi di Napoli Federico II, I-80125 Napoli, Italy*
[2]*DICEM Università di Cassino e del Lazio Meridionale, Italy*
[3]*CNR-SPIN Institute of Superconductors, Innovative Materials and Devices, I-80078 Pozzuoli, Italy*
[4]*Qunatech srl, via Giacinto Gigante 174, 80128 Napoli, Italy*
[5]*Photon Technology Italy srl, via Giacinto Gigante 174, 80128 Napoli, Italy*
[6]*Shanghai Key Laboratory of Superconductor Integrated Circuit Technology, Shanghai Institute of Microsystem and Information Technology, Chinese Academy of Sciences, Shanghai 200050, China*
[*]*pasquale.ercolano@unina.it*

Abstract: Photon-number-resolving superconducting photon detectors promise to simplify detection schemes where only photon statistics matters in the few-photon regimes. Employed in one- and two-photon subtraction protocols, they allowed reconstruction of the photon number distribution for coherent and thermal states obtained from a pulsed laser at telecom wavelengths. The experimental setup is based on photon detection events recorded using a photon-number-resolving detector based on an array of eight superconducting NbN nanostrips working at 2.2 K. Photon subtraction was implemented using a low-reflectivity beam splitter and two superconducting nanostrip single photon detectors with an efficiency higher than 90% and a dark count rate of 1 cps. Our results confirm that our scheme accurately reproduces the theoretically expected effects of the annihilation operator on the states, achieving a fidelity higher than 99%.

1. Introduction

A detector capable of resolving the number of photons is a powerful device in quantum information optical protocols. On one hand, quantum key distribution [1], quantum random number generation [2], linear optics quantum computing [3], have all fostered the rapid advancement of photon-number-resolving detectors (PNRDs) [4–6]. On the other hand, increasing PNRDs performances has widened their application to n-photon state experiments [7], and detectors and photon sources calibration [8]. These advancements are indeed related to preparing, manipulating and characterizing quantum states of light, which are at the base of optical quantum technologies [9]. In particular, PNRDs may experimentally realize, in a single detector, repeated actions of the annihilation operator on a quantum state or directly sample the photon statistics [10,11]. Thus, contrarily to setups where only single photon detectors are employed, PNRDs embody in a single object state manipulation and characterization. Here, we aim at showing the reliability and the high performances of an eight-pixel PNRD, composed of eight superconducting NbN nanostrips operating at 2.2 K, in such a scenario. Superconducting nanostrip detectors, indeed, show near-unit detection efficiency at 1550 nm with a low dark count rate [12].

Photon subtraction has been realized in different experiments. First of all, the annihilation operator was applied to a laser at 786 nm using avalanche photodiodes [10,13]. The state was then reconstructed through homodyne detection, demonstrating the invariance of the coherent state upon photon subtraction, as well as the increase in the average photon number when applied

#568296 https://doi.org/10.1364/OE.568296
Journal © 2025 Received 20 May 2025; revised 23 Jun 2025; accepted 23 Jun 2025; published 30 Jul 2025

Optics EXPRESS

to pseudothermal light generated by a rotating diffuser. Since the appearance of superconducting nanostrip single photon detectors (SNSPDs) [14], it has been clear that they could have represented a breakthrough for the realization of efficient photon subtractions and for moving to longer wavelengths that are requested for actual communication networks and ground to satellite quantum links [15–17]. Morin *et al.* used a SNSPD to achieve photon subtraction from a squeezed vacuum state at 1064 nm [15]. More recently, Melalkia *et al.* demonstrated photon subtraction from a squeezed vacuum state at 1560.44 nm employing a SNSPD [18]. However, multi-photon subtraction requires the employment of a PNRD. A one- and two-photon subtracted squeezed vacuum state was generated at 1560 nm by Namekata *et al.* using a transition-edge sensor (TES) [11]. In the latest development, Endo *et al.* achieved the subtraction of three and four photons from a squeezed vacuum state at 1550 nm with a TES [19,20]. All these experiments used an auxiliary homodyne detector playing the role of state characterisation stage.

However, experiments involving pulsed light present greater challenges compared to the ones with continuous wave light, as they require precise matching of spatial and temporal modes in pulse homodyne detection [19,21]. A less complex experimental method for the characterization of photon-subtracted states is directly employing a PNRD also for quantum state characterization. This approach is particularly suitable when photon statistics is the only requested characteristic. For instance, this was demonstrated by Allevi *et al.* using two hybrid photodetectors at a wavelength of 523 nm [22], and by Zhai *et al.* employing two TES at 850 nm [23]. However, although TES detectors can resolve the number of photons with high efficiency, they suffer from a long (~μs) recovery time [24,25]. Conversely, SNSPD arrays can resolve photon numbers efficiently with nanosecond recovery times and operate at higher, more accessible temperatures (~1 K), unlike TES, which require ~100 mK and have slower recovery times [25–27].

In this study, we focus on an experimental setup utilizing an eight-pixel PNRD composed of eight superconducting NbN nanostrips operating at 2.2 K. In our detector, each pixel contributes equally to the overall detection efficiency as, thanks to the interleaved geometry, the incoming light uniformly illuminates the eight nanostrips [28]. This allows for a simple modelling of the detector's response using a matrix [29]. This kind of detectors enables the characterization of quantum states based on photon detection events, providing a reliable method for reconstructing the photon number distribution [28]. We tested its performance through the implementation of the photon annihilation operator and its application to two distinct quantum states, coherent and thermal, at telecom wavelength. The ability to modify the coherent photon number distribution to a thermal one is achieved through the introduction of a rotating disk [30]. In addition, the annihilation operator is obtained using a low-reflectivity beam splitter (BS) and two SNSPDs with efficiency higher than 90% and a dark count rate of 1 cps. This setup ensures that the effects of the annihilation operator on the quantum states are accurately captured, allowing us to achieve a fidelity higher than 99%. Therefore, we demonstrate the reliability of superconducting nanostrip PNRDs in directly measuring the statistical properties of few-photon light beams, testing them in one- and two-photon subtraction protocols. The superconducting detectors used in this experiment allow for the rapid subtraction of photons and state reconstruction, thanks to their nanosecond recovery time that is shorter than the typical one of TES [23]. Moreover, operating at higher temperatures, PNRDs require simpler cryogenic systems. Specifically, we work with a pulsed laser at 1550 nm with a repetition rate of 20 MHz. Our results confirm the theoretical predictions regarding the effects of the annihilation operator on the photon number distribution of simple quantum states. We demonstrate that the annihilation operator has no effect on a coherent state, while it doubles the mean photon number per pulse if applied to a thermal state and triples the same mean if it is applied twice. In this way, we demonstrate the practical application of PNRDs in experiments where accurate knowledge of photon statistics is crucial.

Optics EXPRESS

2. Quantum measurement model

Superconducting nanostrip PNRDs are able to detect up to N photons simultaneously arriving at the detector, where N is the number of strips of the detector. To model the full experimental setup, we start from the diagonal elements of a generic state density matrix in the Fock representation. Off-diagonal terms are not interesting for statistically characterising the state in terms of the photon number, which represents the final quantity the PNRD will detect. The state's density matrix diagonal entering the subtraction protocol is:

$$\hat{\rho} = \sum_{n=0}^{\infty} \rho_n |n\rangle\langle n| \tag{1}$$

and it is then transformed by a BS with transmissivity T and reflectivity R, into:

$$\hat{\rho}_{ab} = \sum_{n=0}^{\infty} \sum_{k=0}^{n} \rho_n \frac{n!}{k!(n-k)!} T^{n-k} R^k |n-k\rangle_a |k\rangle_{b\,b} \langle k|_a \langle n-k| \tag{2}$$

where the subscript a corresponds to the BS transmission port and b corresponds to the reflection port. We can write the state on mode a conditioned by the number of photons detected in mode b using a positive operator-valued measure (POVM). In the case of a v-photon detection, its expression is:

$$\hat{\Pi}_v = \sum_{i=0}^{\infty} \sigma_{vi} |i\rangle\langle i| \ , \tag{3}$$

where σ is the response matrix of the detector on mode b. In particular, σ_{vi} is the probability that the detector registers v detection events when i photons arrive. In the case of an array of equally illuminated N identical detectors of quantum efficiency η, its expression is [29]:

$$\sigma_{vi} = \begin{pmatrix} N \\ v \end{pmatrix} \sum_{j=0}^{v} (-1)^j \begin{pmatrix} v \\ j \end{pmatrix} \left[(1-\eta) + \frac{v-j}{N} \eta \right]^i . \tag{4}$$

We note that the factor $1/N$ comes from the fact that if a photon enters the array, it has the chance $1/N$ to reach one of the detectors. Then, the conditioned state for single photon detection on mode b is:

$$\hat{\rho}'_a = \frac{Tr_b(\hat{\rho}_{ab}\hat{\Pi}_1)}{Tr(\hat{\rho}_{ab}\hat{\Pi}_1)} \ , \tag{5}$$

where Tr_b indicates the partial trace on mode b and it reads:

$$Tr_b(\hat{\rho}_{ab}\hat{\Pi}_1) = \sum_{n=0}^{\infty} \sum_{k=0}^{n} \rho_n \sigma_{1k} \frac{n!}{k!(n-k)!} T^{n-k} R^k |n-k\rangle_{a\,a} \langle n-k|. \tag{6}$$

Assuming that $R \ll 1$, we can approximate to the first order in R. We also note that $\sigma_{10} = 0$, so the first non-zero term is the one corresponding to $k = 1$:

$$Tr_b(\hat{\rho}_{ab}\hat{\Pi}_1) = \sum_{n=1}^{\infty} \rho_n \sigma_{11} n \ T^{n-1} R |n-1\rangle_{a\,a} \langle n-1|. \tag{7}$$

Since $R \ll 1$, T is very close to 1, and then we can approximate T^{n-1} with 1 for each n, obtaining:

$$Tr_b(\hat{\rho}_{ab}\hat{\Pi}_1) = \sigma_{11} R \sum_{n=0}^{\infty} (n+1) \ \rho_{n+1} \ |n\rangle_{a\,a} \langle n|. \tag{8}$$

Optics EXPRESS

Then, the diagonal of the density matrix for the conditioned state is:

$$\hat{\rho}' = \frac{\sum_{n=0}^{\infty}(n+1)\ \rho_{n+1}|nn|}{\sum_{i=0}^{\infty}(i+1)\ \rho_{i+1}}\ . \tag{9}$$

This state is nothing but the state that can be obtained from applying the annihilation operator to the original one:

$$\hat{\rho}' = \frac{\hat{a}\ \hat{\rho}\ \hat{a}^{\dagger}}{Tr(\hat{a}\ \hat{\rho}\ \hat{a}^{\dagger})}\ . \tag{10}$$

Therefore, under the assumption that $R \ll 1$, detecting an event on the SNSPD is equivalent to applying the annihilation operator.

With the same approximations, we can find that when the detector on mode b does not register detection events, the conditioned state approximates the original one. In addition, when it registers two events, the system mimics applying twice the annihilation operator.

Now, we analyse the action of the PNRD on the mode a represented by $\hat{\rho}$. We make use also in this case of a POVM $\hat{\Pi}_m$ to model the photon detection event distribution recorded by the detector. The probability of recording m detection events is:

$$P_m = Tr(\hat{\rho}\hat{\Pi}_m)\ . \tag{11}$$

To reconstruct the probabilities ρ_n from the distribution of measured events, we use the expectation-maximization-entropy (EME) iterative method developed by Hloušek *et al.* [31], with the initialization condition:

$$\rho_n^{(0)} = \frac{1}{n_{max}+1}\ . \tag{12}$$

Here, n_{max} is the number of terms of the reconstructed distribution, with $n_{max}>\mu$, the average number of photons. The term $\rho_n^{(k)}$ of the distribution, at the generic iteration step k of the algorithm, is:

$$\rho_n^{(k+1)} = \Pi_n^{(k)}\rho_n^{(k)} - \lambda(\ln\rho_n^{(k)} - S^{(k)})\rho_n^{(k)}, \tag{13}$$

where:

$$\Pi_n^{(k)} = \sum_m \frac{P_m\ \sigma_{mn}}{\sum_j \sigma_{mj}\ \rho_j^{(k)}}\ , \tag{14}$$

$$S^{(k)} = \sum_n \rho_n^{(k)} \ln\rho_n^{(k)}. \tag{15}$$

Finally, λ is a scale factor set equal to 10^{-3} as in [31].

3. Experimental setup

The laser source is a fiber-coupled pulsed one at 1550 nm, with a fixed repetition rate 20 MHz. A variable optical attenuator allows to modify the power, and then, the mean photon number per pulse. After that, the light travels through free-space between two ends of SMF28e + fibers. A rotating disk can be placed to modify the photon distribution from Poissonian to Thermal [30]. We used three superconducting photon detectors in a Gifford-McMahon cryostat with a working temperature of 2.2 K. Specifically, we employed a PNRD based on an array of eight superconducting NbN nanostrips of width 75 nm and pitch 180 nm (Fig. 1), each with a dark count rate of 100 cps, recovery time 6 ns, and a total detection efficiency 72%. Indeed, thanks to the interleaved geometry, each strip in the array exhibits the same efficiency because the light is equally divided among them [28]. Since the bias current at the operating point was set to 85% of the critical current, the probability of crosstalk at this level is significant and was therefore neglected [32]. Additionally, we used two SNSPDs, both with DCR = 1 cps and

Optics EXPRESS

detection efficiencies of 92% and 91% respectively. The efficiencies were previously evaluated by a calibrated CW laser at 1550 nm. The fiber was coupled to the chip with the help of an infrared camera at room temperature in order to optimize the coupling efficiency. The polarization was aligned by three-paddle polarization controllers. The detectors were connected to a readout and bias electronic modules. The three detectors' outputs, together with the laser trigger, were sent to a time-to-digital converter. We employed a 99:1 BS after the free-space segment, with the PNRD at the high energy port and the SNSPDs at the other. On the latter side, we arranged a 50:50 BS, which equally divides the 1% component between SNSPD1 and SNSPD2, thus forming an array of two single photon detectors. In this way, we can characterize the photon number distribution without applying the annihilation operator, applying it once, or applying it twice, depending on the detection events on the SNSPDs. A scheme of the experimental setup is sketched in Fig. 2.

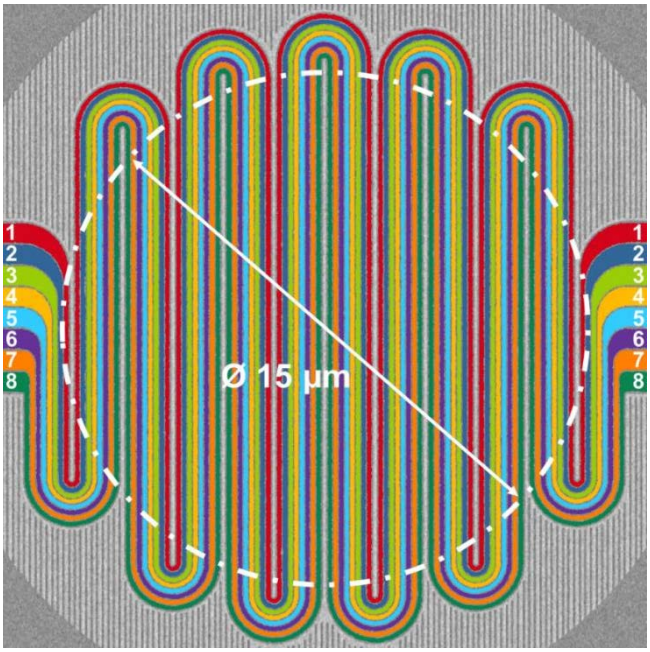

Fig. 1. Scanning electron microscope picture of the eight-pixel superconducting PNRD. Each strip is numbered from 1 to 8 and portrayed in a different colour. The dashed circle indicates the area on which the light from the coupled fiber is focused, with a diameter of 15 µm.

4. Results

We characterized the photon number distribution of the input using the measurements from the PNRD, counting the events at each laser pulse in a time window of 1 ns, and applying the EME method. We measured both with and without the rotating disk, applying or not applying the annihilation operator. For each configuration, we repeated the same measurement at three different attenuations, in each of which we kept the mean number of photons per pulse of about 1. Therefore, since the repetition rate of the laser is 20 MHz, the dark count rate of the PNRD and the one of the SNSPDs can be neglected. As example, we report the reconstructed distributions at a chosen attenuation for the case without disk (Fig. 3(a), 3(b), 3(c)) and with the rotating disk (Fig. 4(a), 4(b), 4(c)).

Optics EXPRESS

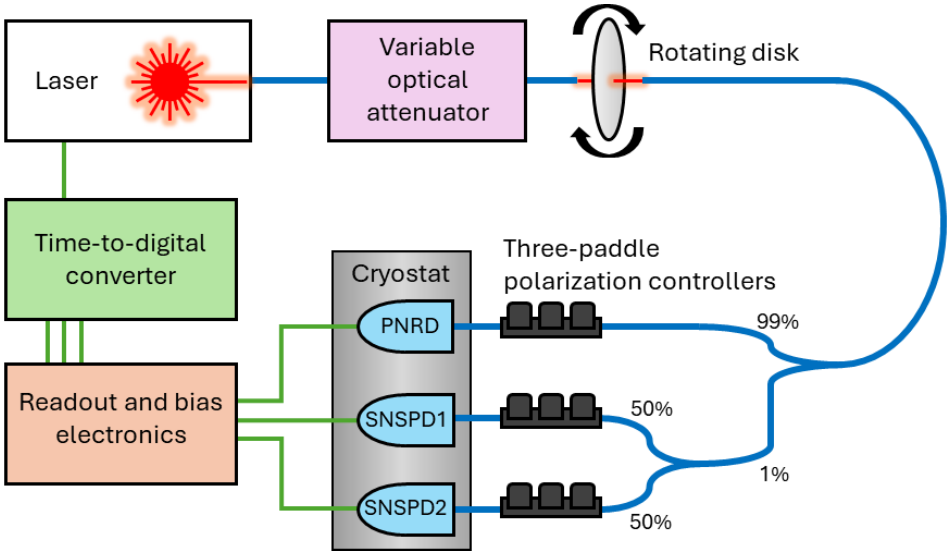

Fig. 2. Schematic of the experimental setup. The power of the 1550 nm pulsed laser is adjusted using a variable optical attenuator. The photon distribution can be modified by a rotating disk. A PNRD records the event distribution, conditioned by the measurements from two SNSPDs. The signals are acquired by a time-to-digital converter.

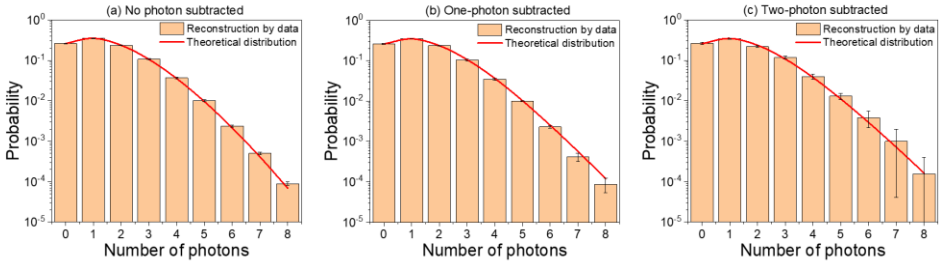

Fig. 3. Photon number distributions reconstructed from data (orange bars) and theoretical Poissonian photon number distributions (red curve) without applying the annihilation operator (a), applying the operator once (b), and applying the operator twice (c).

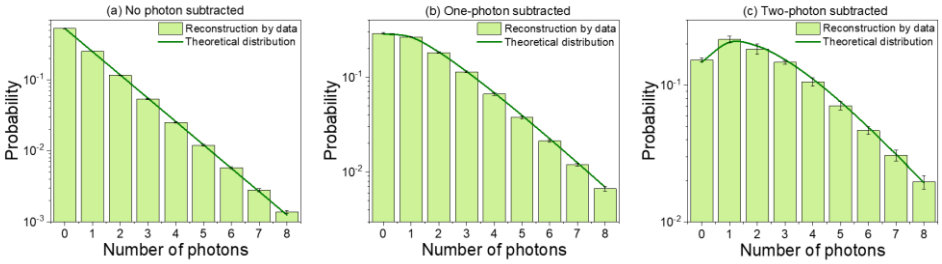

Fig. 4. Photon number distributions reconstructed from data (lime bars) and theoretical Thermal photon number distributions (green curve) without applying the annihilation operator (a), applying the operator once (b), and applying the operator twice (c).

Optics EXPRESS

We denote the mean number of photons per pulse as μ, the second order correlation function as $g^2(0)$, and the fidelity between the reconstructed distribution from the data and the theoretical prediction as F, defined as:

$$F = \left(\sum_n \sqrt{\rho_n^{reconstructed} \rho_n^{theoretical}} \right)^2 . \tag{16}$$

In Table 1 and 2, we use a prime to indicate the quantities related to the distribution obtained by applying the annihilation operator once; two primes indicate its application twice.

Table 1. Experimental results of photon number distributions reconstructed both with and without the rotating disk, both applying the annihilation operator once and not applying it, at three different attenuations.

	μ	$g^2(0)$	F	μ'	$g^2(0)$'	F'
Without disk	1.34 ± 0.01	1.008 ± 0.002	99.997 ± 0.003	1.34 ± 0.03	1.001 ± 0.005	99.987 ± 0.006
	0.82 ± 0.01	1.008 ± 0.003	99.998 ± 0.002	0.83 ± 0.01	1.008 ± 0.004	99.992 ± 0.004
	0.68 ± 0.01	1.008 ± 0.003	99.997 ± 0.003	0.68 ± 0.01	1.008 ± 0.008	99.995 ± 0.005
Rotating disk	0.89 ± 0.01	2.005 ± 0.002	99.981 ± 0.002	1.76 ± 0.03	1.509 ± 0.006	99.884 ± 0.009
	0.70 ± 0.01	2.006 ± 0.002	99.993 ± 0.002	1.38 ± 0.02	1.505 ± 0.006	99.964 ± 0.008
	0.36 ± 0.01	1.998 ± 0.002	99.998 ± 0.002	0.70 ± 0.01	1.502 ± 0.009	99.985 ± 0.009

Table 2. Experimental results of photon number distributions reconstructed both with and without the rotating disk, both applying the annihilation operator twice and not applying it, at three different attenuations.

	μ	$g^2(0)$	F	μ''	$g^2(0)$''	F''
Without disk	1.34 ± 0.01	1.008 ± 0.002	99.997 ± 0.003	1.36 ± 0.03	1.04 ± 0.03	99.87 ± 0.07
	0.82 ± 0.01	1.008 ± 0.003	99.998 ± 0.002	0.83 ± 0.01	0.97 ± 0.05	99.8 ± 0.2
	0.68 ± 0.01	1.008 ± 0.003	99.997 ± 0.003	0.70 ± 0.02	0.96 ± 0.06	99.7 ± 0.1
Rotating disk	0.89 ± 0.01	2.005 ± 0.002	99.981 ± 0.002	2.70 ± 0.04	1.34 ± 0.01	99.46 ± 0.08
	0.70 ± 0.01	2.006 ± 0.002	99.993 ± 0.002	2.09 ± 0.04	1.35 ± 0.02	99.78 ± 0.06
	0.36 ± 0.01	1.998 ± 0.002	99.998 ± 0.002	1.08 ± 0.04	1.37 ± 0.06	99.6 ± 0.1

We show that in the case without disk, the mean number of photons has no measurable differences. Indeed, the coherent state is invariant by single-photon annihilation, and this is confirmed by the high fidelity value. In addition, $g^2(0)$ is almost 1, as expected in a Poissonian distribution.

When the rotating disk is present, resulting in a Thermal distribution, we observe that when the operator is applied once, μ doubles, and when it is applied twice, μ triples, as theoretically predicted. Also $g^2(0)$ values are consistent with the expected 2, 3/2 and 4/3, respectively when the operator is not applied, it is applied once, and it is applied twice. In this case as well, the behaviour of the probabilities related to the photon numbers follows the theoretical predictions, so fidelity values above 99% are obtained in all cases.

Preliminary to the use of the detector in the above setup, we tested it to assess the independence and the equivalence of each nano strip as a single photon detector. This has been conducted realizing one-photon subtraction and photon number statistics characterization using only the PNRD employed above. In this configuration, we treated the signal arriving from a single nanostrip as the triggering single photon detector and used the remaining strips as a PNRD with seven independent nanostrips. In this way, it effectively simulates the light being split between two detectors via a BS. This process can be repeated changing the trigger pixel, resulting in

Optics EXPRESS

eight different configurations. Looking at the results, it is possible to evaluate the splitting ratio between each strip and the others so obtaining an estimation of the illumination uniformity over all the nanostrip.

In these measurements, all the light was directed to the PNRD. For the measurement without the disk (coherent state), the laser was attenuated to achieve $\mu = 1.33 \pm 0.01$, while for the measurement with the rotating disk (thermal state), $\mu = 0.73 \pm 0.01$. We compared all the eight results with the expected theoretical distribution. Figure 5 and 6 report the probabilities for each photon number, using each pixel independently, as well as the expected theoretical distribution for the configurations without the disk and with the rotating disk, respectively. The experimental points obtained by changing the nanostrip that acts as a single photon detector are consistent within the experimental errors. This proves that the detector is uniformly illuminated, and then the probability of detecting a photon is equal for each strip. The fidelity, calculated as in Table 1, for all the different eight cases is always above 99.9%.

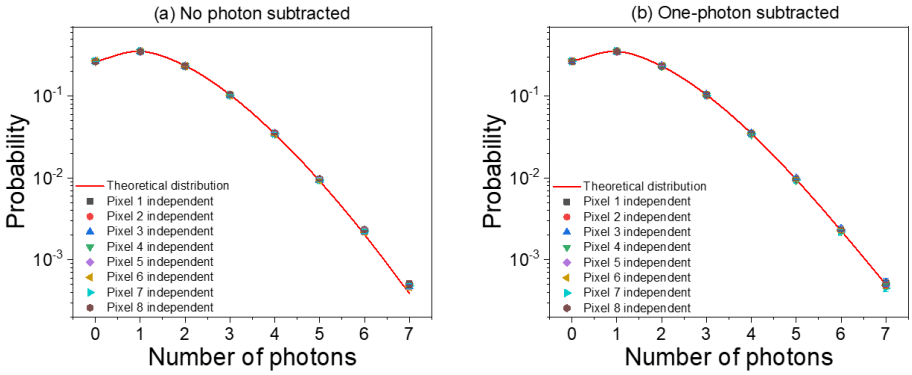

Fig. 5. Photon number distributions reconstructed from data (points), using each pixel as independent, and theoretical Poissonian photon number distributions (red curve) without applying the annihilation operator (a) and applying the operator once (b). Experimental points are completely indistinguishable, thus proving that the behaviours of all nanostrips are completely equivalent.

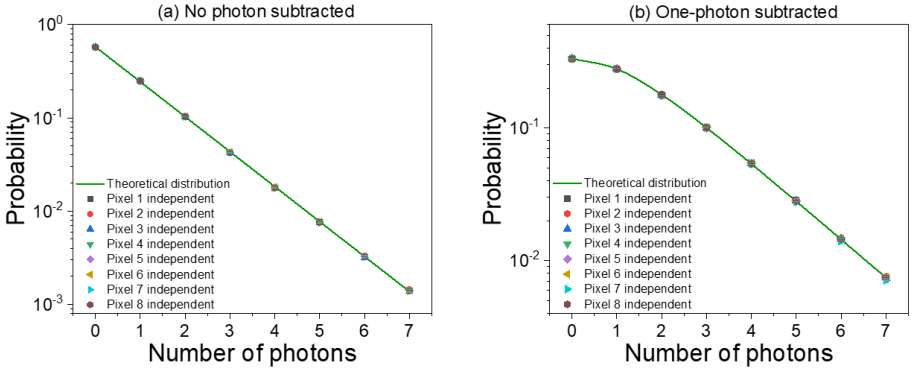

Fig. 6. Photon number distributions reconstructed from data (points), using each pixel as independent, and theoretical Thermal photon number distributions (red curve) without applying the annihilation operator (a) and applying the operator once (b). Experimental points are completely indistinguishable, thus proving that the behaviours of all nanostrips are completely equivalent.

Optics EXPRESS

5. Conclusion

Superconducting nanostrip PNRDs represent a key device for the realization of different quantum information protocols, thanks to their recovery time of few ns and their very low dark count rate. Here, we have employed a PNRD in a one- and two-photon subtraction protocol at 1550 nm. We have illuminated the PNRD with the heralded one and two photons subtracted state, thus allowing a direct access to the photon statistics of coherent and thermal states in the few-photon regime. The method avoids the complexity of using homodyne detection. We verified the effects on the photon number distributions of photon subtraction, through a simple experimental setup involving high-efficiency superconducting nanostrip single photon detectors operating at 2.2 K. Our results, in full agreement with the expected behaviour, demonstrate the possibility of reaching high repetition rates in quantum information protocols where the knowledge of photon distributions is essential. We performed this measurement using a laser with a fixed repetition rate of 20 MHz, but the superconducting PNRD recovery time of 6 ns could allow higher repetition rates.

Funding. European Commission (101091408); Università degli Studi di Napoli Federico II (E63C24002560005); Ministry of Science and Technology of the People's Republic of China (2023ZD0300100).

Disclosures. The authors declare no conflicts of interest.

Data availability. Data underlying the results presented in this paper are not publicly available at this time but may be obtained from the authors upon reasonable request.

References

1. W. Lei, L. Zhang, H. Tan, *et al.*, "High-rate quantum key distribution exceeding 110 Mb s–1," Nat. Photonics **17**(5), 416–421 (2023).
2. P. Ercolano, M. Ejrnaes, C. Bruscino, *et al.*, "Superconducting Nanostrip Photon-Number-Resolving Detector as an Unbiased Random Number Generator," IEEE Trans. Quantum Eng. **5**, 4100808 (2024).
3. E. Knill, R. Laflamme, and G. J. Milburn, "A scheme for efficient quantum computation with linear optics," Nature **409**(6816), 46–52 (2001).
4. J. Provazník, L. Lachman, R. Filip, *et al.*, "Benchmarking photon number resolving detectors," Opt. Express **28**(10), 14839–14849 (2020).
5. T. Zhang, J. Huang, X. Zhang, *et al.*, "Superconducting single-photon detector with a speed of 5 GHz and a photon number resolution of 61," Photonics Res. **12**(6), 1328–1333 (2024).
6. P. Li, J. Zhong, W. Zhang, *et al.*, "High-Performance Ti Transition-Edge Sensor-based Photon-Number Resolving Detectors," J. Low Temp. Phys. **214**(3-4), 100–105 (2024).
7. A. Divochiy, F. Marsili, D. Bitauld, *et al.*, "Superconducting nanowire photon number resolving detector at telecom wavelength," Nat. Photonics **2**(5), 302–306 (2008).
8. A. L. Migdall, D. Branning, and S. Castelletto, "Tailoring single-photon and multiphoton probabilities of a single-photon on-demand source," Phys. Rev. A **66**(5), 053805 (2002).
9. N. Biagi, S. Francesconi, A. Zavatta, *et al.*, "Photon-by-photon quantum light state engineering," Prog. Quantum Electron. **84**, 100414 (2022).
10. V. Parigi, A. Zavatta, M. Kim, *et al.*, "Probing quantum commutation rules by addition and subtraction of single photons to/from a light field," Science **317**(5846), 1890–1893 (2007).
11. N. Namekata, Y. Takahashi, G. Fujii, *et al.*, "Non-Gaussian operation based on photon subtraction using a photon-number-resolving detector at a telecommunications wavelength," Nat. Photonics **4**(9), 655–660 (2010).
12. L. You, "Superconducting nanowire single-photon detectors for quantum information," Nanophotonics **9**(9), 2673–2692 (2020).
13. A. Zavatta, V. Parigi, M. S. Kim, *et al.*, "Subtracting photons from arbitrary light fields: experimental test of coherent state invariance by single-photon annihilation," New J. Phys. **10**(12), 123006 (2008).
14. G. N. Gol'tsman, O. Okunev, G. Chulkova, *et al.*, "Picosecond superconducting single-photon optical detector," Appl. Phys. Lett. **79**(6), 705–707 (2001).
15. O. Morin, K. Huang, J. Liu, *et al.*, "Remote creation of hybrid entanglement between particle-like and wave-like optical qubits," Nat. Photonics **8**(7), 570–574 (2014).
16. C. Bruscino, P. Ercolano, D. Salvoni, *et al.*, "High Performance Superconducting Nanowire Single Photon Detectors for QKD Applications," IEEE Trans. Appl. Supercond. **34**(3), 1–5 (2024).
17. H. Hao, Q. Zhao, Y. Huang, *et al.*, "A compact multi-pixel superconducting nanowire single-photon detector array supporting gigabit space-to-ground communications," Light: Sci. Appl. **13**, 25 (2024).
18. M. F. Melalkia, T. Gabbrielli, A. Petitjean, *et al.*, "Plug-and-play generation of non-Gaussian states of light at a telecom wavelength," Opt. Express **30**(25), 45195–45201 (2022).

Optics EXPRESS

19. M. Endo, R. He, T. Sonoyama, *et al.*, "Non-Gaussian quantum state generation by multi-photon subtraction at the telecommunication wavelength," Opt. Express **31**(8), 12865–12879 (2023).
20. M. Endo, T. Nomura, T. Sonoyama, *et al.*, "High-Rate Four Photon Subtraction from Squeezed Vacuum: Preparing Cat State for Optical Quantum Computation," arXiv (2025).
21. Z. Qin, A. S. Prasad, T. Brannan, *et al.*, "Complete temporal characterization of a single photon," Light: Sci. Appl. **4**(6), e298 (2015).
22. A. Allevi, A. Andreoni, M. Bondani, *et al.*, "Reliable source of conditional states from single-mode pulsed thermal fields by multiple-photon subtraction," Phys. Rev. A **82**(1), 013816 (2010).
23. Y. Zhai, F. E. Becerra, B. L. Glebov, *et al.*, "Photon-number-resolved detection of photon-subtracted thermal light," Opt. Lett. **38**(13), 2171–2173 (2013).
24. M. Eaton, A. Hossameldin, R. J. Birrittella, *et al.*, "Resolution of 100 photons and quantum generation of unbiased random numbers," Nat. Photonics **17**(1), 106–111 (2023).
25. A. E. Lita, D. V. Reddy, V. B. Verma, *et al.*, "Development of superconducting single-photon and photon-number resolving detectors for quantum applications," J. Lightwave Technol. **40**(23), 7578–7597 (2022).
26. W. Zhang, J. Huang, C. Zhang, *et al.*, "A 16-Pixel Interleaved Superconducting Nanowire Single-Photon Detector Array With A Maximum Count Rate Exceeding 1.5 GHz," IEEE Trans. Appl. Supercond. **29**(5), 1–4 (2019).
27. J. X. Chen and H. Li, "Research progress of high speed superconducting nanowire single-photon detector," Journal of Functional Materials and Devices **31**(1), 1–10 (2025).
28. P. Ercolano, C. Bruscino, D. Salvoni, *et al.*, "Time Binning Method for Nonpulsed Sources Characterization With a Superconducting Photon Number Resolving Detector," IEEE Trans. Quantum Eng. **4**, 4100609 (2023).
29. M. J. Fitch, B. C. Jacobs, T. B. Pittman, *et al.*, "Photon-number resolution using time-multiplexed single-photon detectors," Phys. Rev. A **68**(4), 043814 (2003).
30. F. T. Arecchi, "Measurement of the statistical distribution of Gaussian and laser sources," Phys. Rev. Lett. **15**(24), 912–916 (1965).
31. J. Hloušek, M. Dudka, I. Straka, *et al.*, "Accurate detection of arbitrary photon statistics," Phys. Rev. Lett. **123**(15), 153604 (2019).
32. G. V. Resta, L. Stasi, M. Perrenoud, *et al.*, "Gigahertz detection rates and dynamic photon-number resolution with superconducting nanowire arrays," Nano Lett. **23**(13), 6018–6026 (2023).